Talanta 105 (2013) 333–339

Contents lists available at SciVerse ScienceDirect

Talanta

journal homepage: www.elsevier.com/locate/talanta

Inkjet-printed polyaniline patterns for exocytosed molecule detection from live cells

Wan-Kyu Oh, Sojin Kim, Kyoung-Hwan Shin, Yongjin Jang, Moonjung Choi, Jyongsik Jang *

World Class University (WCU) program of Chemical Convergence for Energy & Environment (C_2E_2), School of Chemical and Biological Engineering, Seoul National University, 599 Gwanangro, Gwanak-gu, Seoul 151–742, Korea

ARTICLE INFO

Article history:
Received 26 April 2012
Received in revised form
13 October 2012
Accepted 15 October 2012
Available online 23 October 2012

Keywords:
Inkjet printing
Conducting polymers
Bioelectronics
Biosensors
Exocytosis

ABSTRACT

Polyaniline (PANi) patterns on flexible substrate are fabricated for biomolecule detection from live cells. PANi patterns are prepared by inkjet printing on polyethylene terephthalate film. Subsequently, arginine–glycine–aspartate (RGD) peptide is immobilized on the PANi pattern to selectively adhere cells. Rat pheochromocytoma PC12 cells are cultured on the RGD–immobilized PANi pattern, and patterned with high selectivity and growth. Additionally, the cells show focal adhesion on the RGD–immobilized PANi pattern, which are confirmed with vinculin staining and scanning electron microscopic images. To monitor dynamic biomolecular release from PC12 cells, RGD–immobilized PANi pattern is used for a real-time electrical signal detector. RGD–immobilized PANi patterning and sensing system represents outstanding ability to translate and amplify exocytosis molecules into a detectable signal as a transducer.

1. Introduction

Conducting polymers (CPs) have attracted considerable attention given their potential to produce flexible, biocompatible, and light-weight devices, as alternatives to inorganic semiconductors or metals [1–3]. Recent progress in the synthesis of CPs has overcome several interfacial problems in the field of organic bioelectronics such as the application of tissue–electrode interfaces for nerve regeneration, biorecognition, and the preparation of cell–electrode interfaces for multifunctional neuron probes [4–6]. Biocompatible CP electrodes have prompted to apply biointerfaces for enhancing cell–electrode communication, markedly in nervous systems for their patterning and recording functionalities. CPs are readily tailored by surface modification or doping method ranging from small ions to macromolecules [7–9].

Inkjet printing is an efficient alternative to conventional photolithography for the production of versatile CP–based micro/nanoelectronic devices owing to its low cost, high–speed patterning, flexibility, shape control, and applicability to various substrates [10–12]. Recently, inkjet printing has been reported as a promising candidate for bio-applications due to its facile and versatile micro-patterning of biomaterials, however, relatively little research has been carried out on biomedical fields [13,14].

Surface patterning is routinely used to immobilize bioactive molecules such as proteins, oligonucleotides and small ligands; to localize surface reactions for bioassays; and to provide cell and bacterial adhesion [15,16]. Such patterning is exploited for biochips, co–cultures, tissue engineering, cell–based biosensors, and studies of extracellular effects on cell behavior [17–19]. Cell adhesion plays a crucial role in many biological processes, including cell guidance, wound repair, and extracellular signal transduction [20,21]. When cells adhere to the extracellular matrix (ECM) *via* cell surface receptors, integrins mediate signal transduction pathways that influence a range of cellular processes [22]. Cell adhesion to substrate via transmembrane cell receptors has been mostly controlled by short and simple peptide sequences. The modification of substrates with ECM proteins provides cell-attachable surfaces [23]. As cell attachment to the substrate depends on the type of ECM protein and on the subset of integrin receptors present on a specific cell type, the choice of immobilized proteins provides selectivity for specific immobilization of certain cell types. The first peptide developed to the ECM protein fibronectin was the tripeptide Arg–Gly–Asp (RGD) in 1984 [24]. This tripeptide is the minimal recognition sequence for integrin receptors. Peptides containing the RGD sequence induce the adhesion of many cell types including fibroblasts, osteoblasts and macrophages [25]. Besides the RGD sequence other cell recognition motifs exist, but only some of them have been immobilized for cell attachment so far [26]. The RGD sequence is by far the most effective and most often employed peptide sequence for stimulated cell adhesion on synthetic surfaces.

* Corresponding author. Fax: +82 2 888 7295.
E-mail address: jsjang@plaza.snu.ac.kr (J. Jang).

0039-9140/$ - see front matter © 2012 Elsevier B.V. All rights reserved.
http://dx.doi.org/10.1016/j.talanta.2012.10.050

The recording of electrical signals from cells and tissues is central to areas ranging from fundamental biophysical studies (*e.g.*, heart and brain) to medical monitoring and intervention [27,28]. Over the past few decades, a large effort has been devoted to recording signals from electroactive cells [29,30]. Many studies have focused on the field effect transistors method, which uses inorganic nanowires and carbon nanotubes to produce recording with a high signal–to–noise ratio from electroactive cells [31,32]. However, these materials do not guarantee selective cell adhesion because of their intrinsic properties such as inert surface, cellular toxicity, modification difficulties [2]. The control of material–cell surface interactions is key for a wide range of biomedical applications [33]. To allow cells to adhere to the pattern, bioactive ligands must allow the cell to interact with extracellular matrix proteins or structurally related synthetic peptides [34].

Here we fabricated flexible inkjet-printed polyaniline (PANi) patterns for selective cellular patterning and the electrical detection of biomolecules. The PANi pattern was prepared by oxidant inkjet printing on poly(ethylene terephthalate) (PET) film with subsequent vapor deposition polymerization of aniline monomers. RGD peptide was then grafted onto the PANi pattern as a simple method for selectively binding live cells. The detection of electrical biomolecule from neurons was performed using an interdigitated microelectrode array. Several features of such a multifunctional PANi pattern make it particularly attractive for patterning and sensing neuronal cells, including: (1) the simplicity of fabricating precise micro–sized cell patterns; (2) facile modification for the grafting RGD peptide *via* covalent bonding with PANi; (3) focal adhesion between cells and the PANi pattern; (4) the flexibility of the substrate, which makes it applicable to various biomedical fields; and (5) the electrical detection of biomolecule secretion from live cells to allow studies at the subcellular level.

2. Materials and methods

2.1. Patterning of polyaniline (PANi)

Ammonium persulfate (APS; 98%), purchased from Sigma-Aldrich Co. Ltd. (St. Louis, MO, USA), was used as an oxidant. Aniline monomer (99%) was obtained from Sigma-Aldrich Co. Ltd. and used without further purification. PET (3M) film was used as a substrate for inkjet printing. Commercial office inkjet printer (Canon Pixma IP1300) was purchased and modified for this work. The ink cartridge (printer head) was disassembled and washed several times with ethanol and distilled water after removal of the ink. An oxidant solution containing 1.18 M APS in distilled water was injected into the modified ink cartridge. The completely sealed cartridge was subsequently placed in the printer body and prepared for use. For PANi patterning, the complexly patterned architectures were designed in advance using a computer software package (Microsoft PowerPoint 2003). The oxidant APS solution was printed onto PET film in the desired pattern using the modified inkjet printer. The printed film was then cut and placed in a vapor phase polymerization (VDP) chamber (70 °C) containing aniline monomer (4 mL) and 0.1 M hydrochloric acid solution (1 mL) for 15 min. Emeraldine salt form of PANi patterns were formed in the VDP chamber at 70 °C. Fig. S1 shows a schematic diagram of our inkjet printing procedure.

2.2. RGD peptide immobilization

The printed patterns were washed with distilled water twice to remove residual APS. The printed patterns were treated with 0.5% glutaraldehyde solution for 2 h. The patterns were then thoroughly washed with distilled water and immersed in pure ethanol to remove adsorbed molecules from the substrate. The aldehyde presenting pattern was incubated with 0.5 mM amine terminated GRGDS peptide solution in PBS buffer for 1 h at 37 °C. After incubation, the pattern was washed three times with 0.1 M PBS. The patterns were reacted with EDC for 2 h and then incubated with NHS and 0.5 mM amine terminated GRGDS peptide solution in PBS buffer for 1 h at 37 °C. After incubation, the pattern was washed three times with 0.1 M PBS. As a control, poly(ethylene glycol) (PEG, molecular weight *Mw* ~5,000) modification was conducted on the PANi pattern. 1 mM PEG-succinimidyl ester (NANOCS Inc, MA, USA) solution was added in the PANi pattern for 1 h at 37 °C. After incubation, the pattern was washed three times with 0.1 M PBS.

2.3. Cell culture

PC–12 cells obtained from the American Type Culture Collection (Manassas, VA, USA) were maintained in RPMI-1640 with 10% fetal bovine serum, 1% penicillin–streptomycin solution, 25 mM sodium bicarbonate, 300 mg L^{-1} L–glutamine, and 25 mM 4–(2-hydroxyethyl)–1–piperazine ethansulfonic acid (HEPES) at 37 °C in a 5% CO_2 atmosphere in 75–cm^2 flasks. The cells were subcultured three times per week. All experiments were performed in a clean atmosphere.

2.4. Observation of live PC–12 cells on RGD-immobilized PANi pattern

PC-12 cells (2×10^4) were cultured on an RGD-immobilized PANi substrate in 24-well plates (Nunc, Thermo Fisher Scientific, Rochester, NY, USA). After 48 h, the medium was removed and the cells were washed twice with 0.1 M PBS. The cells were then stained with 1 μM cell tracker probe solution (Molecular Probes, Invitrogen, Carlsbad, CA, USA) for 30 min at 37 °C. The probe solution was then replaced with pre-warmed medium and the cells were incubated for another 30 min at 37 °C. The cells were then washed twice with 0.1 M PBS and fixed in 3.7% paraformaldehyde for 15 min at 25 °C. The cells fixed on the RGD-patterned PANi substrates were analyzed with a Delta Vision® RT imaging system (Applied Precision, Issaquah, WA, USA) under 5% CO_2 at 37 °C. To obtain images, a Cascade II electron multiplying charge-coupled device (EMCCD) camera was used.

2.5. Immunofluorescence staining of PC–12 cells

PC–12 cells, grown under the conditions described above, were fixed in 4% paraformaldehyde for 10 min, permeabilized in 0.5% Triton X–100 for 5 min, and then blocked in PBS containing 4% bovine serum albumin, and 0.01% sodium azide for 15 min. To detect focal adhesion, FITC–tagged monoclonal anti–vinculin antibodies (Sigma-Aldrich Co. Ltd.) was used. To characterize the cytoskeleton morphology, rhodamine–phalloidin (Cytoskeleton) labeling (100 nM in PBS from a 1 mg mL^{-1} methanol stock solution) was used. After washing, the nuclei were stained and the samples were mounted on a glass coverslip using Fluoroshield (Sigma) and characterized using a Delta Vision® RT imaging system (Applied Precision). The samples were observed at 40 × using the 1.515 N.A. oil immersion objective.

2.6. Imaging of PC-12 cells on the RGD–immobilized PANi pattern by SEM

The morphology of cells on the RGD-immobilized PANi pattern was determined by SEM (SUPRA 55VP, Carl Zeiss, Jena, Germany). Cells (2×10^4 mL^{-1}) were cultured on RGD-immobilized PANi patterns for 48 h, then washed twice with cold 0.1 M PBS and

prefixed with 2% paraformaldehyde and 2% glutaraldehyde at 4 °C for 2 h. After being washed three times with 0.1 M PBS, the cells were post-fixed with 1% osmium tetraoxide for 2 h, washed in distilled water, and dehydrated through a graded ethanol series. The dehydrated cells were then dried in a critical point dryer, sputter-coated with platinum, and observed by SEM at an accelerating voltage of 8 kV.

2.7. Sensor substrate

All electrical measurements were conducted with a Wonatech WBCS 3000 potentiostat. A four-well chamber (Lab-Tek™ II, Nunc, Thermo Fisher Scientific) was placed on the PANi substrate for cell culturing and recording. Two electrodes (source and drain) were prepared across the PANi pattern using conductive silver paint. PC-12 cells (2×10^4) were cultured on an RGD-modified PANi substrate in the chamber with 1 mL of medium. After 48 h, the PANi pattern current was monitored at a voltage bias of 50 mV.

3. Results and discussion

Fig. 1 shows a schematic diagram of cell patterning based on the RGD peptide–immobilized PANi pattern. First, oxidant (ammonium persulfate) patterning for polymerization was performed using a modified–commercial inkjet printer. Subsequently, the printed substrate was loaded in the chamber, and aniline monomer was inserted for VDP at 70 °C. Chemical oxidation polymerization of aniline yielded the designed pattern (conductivity: ca. 4 S cm^{-1}). After washing, the substrate was

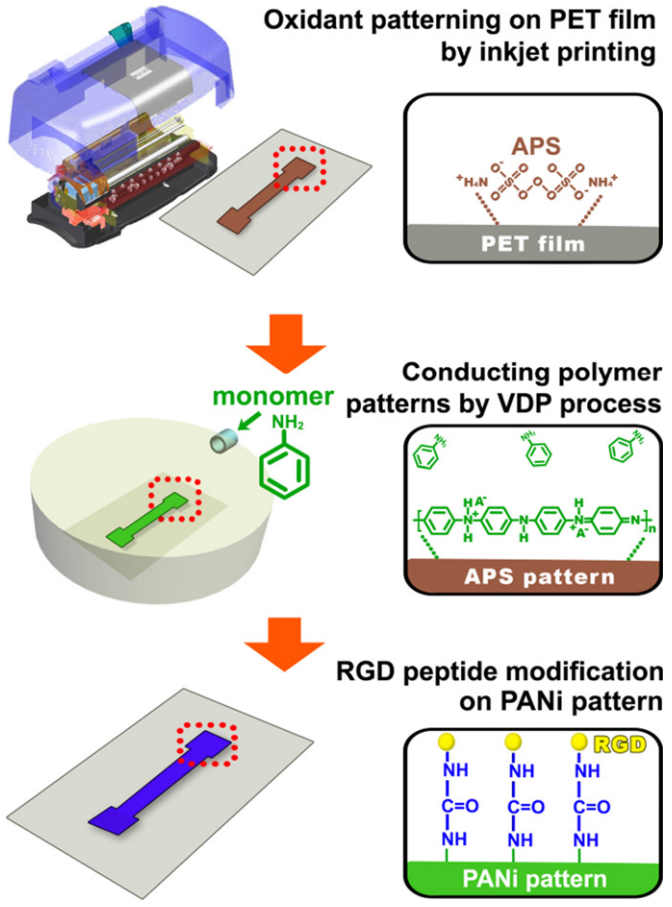

Fig. 1. Schematic illustration of strategy for selective cell patterning via modification of cell binding peptide (RGD peptide) on inkjet-printed PANi.

modified with RGD peptide. The RGD peptide is a fibronectin–derived peptide capable of increasing integrin–mediated cell adhesion and spreading on a variety of substrates *via* its cell–binding domain [29].

To verify successful fabrication of the PANi pattern and RGD peptide binding, Fourier transform infrared (FT–IR) spectra were obtained (Fig. S2). The spectra revealed that PANi was successfully printed on the PET substrate and that the RGD peptide was successfully grafted onto the PANi pattern. The FT–IR spectrum of PANi pattern (black line) exhibited characteristic peaks of PANi, including an out–of–plane bending vibration of C–H on para-disubstituted rings at 845 cm^{-1}, a stretching vibration due to a C═C quinonoid ring at 1481 and 1125 cm^{-1}, and a stretching vibration of C–N at 1257 cm^{-1} [30]. This result demonstrates the successful polymerization of PANi on the PET film by inkjet printing. In the case of RGD peptide immobilization (red line), the peaks related to imine and C–N stretching increased after RGD immobilization (1692 and 1400 cm^{-1}, respectively), while the N–H deformation peak at 1320 cm^{-1} decreased [35,36]. These findings indicate that the RGD peptide was grafted onto the PANi pattern. Scanning electron microscopy (SEM) revealed high–resolution PANi pattern and smooth edge waviness did not impact the connections (Fig. 2a). Additionally, pristine PANi pattern exhibits smooth surface which is caused by VDP (Fig. S3). The roughness of the PANi pattern increased, as shown by SEM, confirming attachment of the RGD peptide (Fig. S3). Furthermore, the line width was controlled in the range of 50–1000 μm, indicating successful generation of software–guided automatic patterning.

Fig. 2b and c show representative images of PC12 cell patterning on the inkjet-printed PANi. As shown by SEM and fluorescence microscopic images, cells were selectively grown on the PANi pattern. It is known that PET films do not show affinity for cells, whereas RGD peptide-treated PANi pattern shows high affinity toward cells [37]. This methodology demonstrated wide–range selective cell attachment on the PANi pattern (Fig. S4). Most PC12 cells were located on the PANi pattern with high selectivity. Furthermore, cell proliferation and selectivity increased with an increase in RGD peptide concentration (Fig. 3a). As the RGD peptide concentration increased from 0 to 1 mM, the selectivity increased from ca. 2.0–15.4 after 48 h, which was appropriate for cell patterning. Furthermore, the cell numbers on the pattern increased after RGD modification of its surface, from 334 cells on the pristine PANi to 313 cells on the PEG–treated PANi and 1067 cells on a 1 mM–RGD–immobilized PANi pattern (Fig. 3b). As a control, PEG modification was conducted on the PANi pattern (see Materials and Methods). In the case of the PEG-treated PANi pattern, surface functionality of the pattern enabled to decrease cellular attachment although the roughness of the pattern increased compared with pristine PANi pattern (Fig. S3). Judging from these data, the RGD peptide–immobilized PANi pattern enabled selective PC12 cell patterning. Therefore, this system may be used for neuron patterning and sensing. Several relative results have been demonstrated using PANi-based materials for on-chip cell manipulation. For example, PANi-coated polymer nanofibers have been used to evaluate the electrical stimulation of neuron extension on the nanofibers; a hybrid polymer platform consisting of biodegradable polymer fibers aligned on conductive polypyrrole doped toluenesulfonate promotes directionally controlled axonal growth and accelates nerve growth [38,39].

To investigate the focal adhesion of PC12 cells on the PANi pattern, we explored the distribution and recruitment of vinculin, the expressed cytoskeletal protein. Vinculin is related to the plaques characteristic of focal adhesion complexes [40]. Fig. 4 displays fluorescence microscopic images of PC12 cells on different PANi patterns. For each patterns, an overlay of vinculin

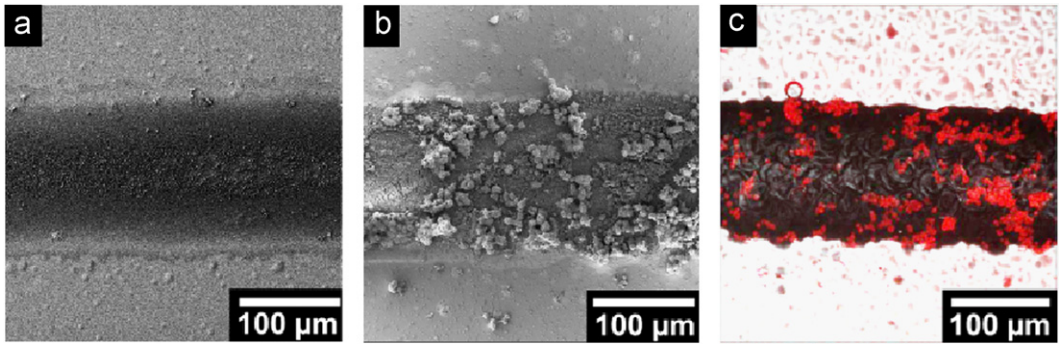

Fig. 2. SEM images of (a) pristine PANi pattern and (b) PC–12 cells on the RGD-immobilized PANi pattern. (c) Representative differential interference contrast (DIC) image of PC–12 cells on the RGD–immobilized PANi pattern.

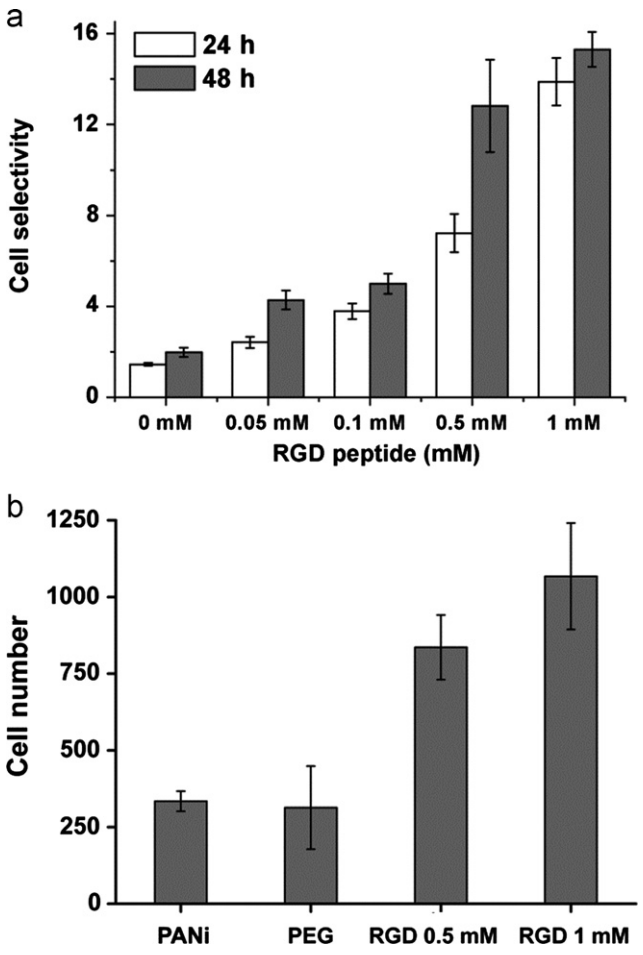

Fig. 3. (a) PC–12 cell selectivity of PANi pattern with respect to increasing concentration of the RGD peptide. Cell selectivity was calculated with counting cells on PANi pattern compared with cells on PET substrate. (b) PC–12 cell number on PANi pattern with respect to surface modifications (pristine PANi pattern, PEG treatment, and RGD peptide-modification). Cells were counted on the 10x microscopic images. Values exhibit mean ± SD and each experiment was performed in triplicate.

(green), actin (red), and the nucleus (blue) is shown, together with separate images stained for vinculin, actin, and the nucleus. Cells on pristine and PEG–treated PANi patterns were spherical and mostly localized (Fig. 4a and b). Small spots can be seen in the vinculin stained images, but vinculin is localized mainly in the cytoplasm. Few focal complexes or nascent adhesions could be seen on the surface of the cells in the pristine PANi pattern. These complexes are thought to be transient structures that can transform into focal adhesions at the lamellar edge and mature to link with actin stress fibers [41]. The cells on RGD–immobilized patterns (Fig. 4c) were spread out significantly more than on the PANi patterns. Vinculin was spread through entire cell, and well–defined vinculin spots were observed in the lamella edge. Significant levels of cellular adhesion were detected, and a proportion of the cells were able to spread and form vinculin–staining complexes. The focal adhesions observed in the RGD–immobilized PANi patterns enabled stronger physical contact with the surface compared to the pristine PANi pattern. Judging from these data, the RGD–peptide plays a critical role in PC12 adhesion and growth.

To observe adhesive complexes at the periphery of PC12 cells, images of fixed cells were obtained by SEM. Fig. 5 shows SEM images of cells adhering to the different surfaces (a: pristine PANi; b: PEG–treated PANi; c and d: RGD–immobilized PANi). Membrane protrusions can be seen extending from the cell body in all images; their size increases as the surface changes from pristine PANi to PEG– and RGD–treated PANi pattern. The cells on RGD–immobilized PANi patterns showed significant adhesion, indicated by the presence of larger focal adhesion (two–digit micrometer). Additionally, cellular morphology differed from that of the cells on the other PANi patterns (they spread out and adhered more to the pattern with focal complexes). It is thought that the RGD ligand enables the development of focal adhesions, leading to spreading, movement, and generation of force. This phenomenon is consistent with previous findings showing that RGD peptide induced the formation of focal adhesions and cell spreading [22,27].

Rat pheochromocytoma PC–12 cells were used as a model to investigate secretion from a live cell, which is related to biological processes such as neurotransmitter secretion from neurons [38]. A secretagogue was used for the detection of secreted molecules from PC12 cells on top of RGD–immobilized PANi patterns (Fig. 6a). To investigate the sensing capability of RGD–immobilized PANi patterns, the current was monitored in real time at $V=50$ mV, a low operating voltage. It is known that voltage-gated calcium ion channel opens via membrane depolarization upon the increment of intracellular potential [28]. A secretagogue is immobilized by the inrush of calcium ions through the channel [28]. As a result, catecholamine molecules (e.g., dopamine, norepinephrine, and epinephrine) inside the vesicle are discharged into the extracellular space [29]. When potassium ions were introduced onto the cells, a train of current spikes was detected (Fig. 6b). When calcymycin was inserted into the pattern, similar current spikes were observed (Fig. 6b). It is believed that the current increase is due to a change in the charge–transport behavior of the PAN is elicited by π–π stacking and hydrogen bonding. The principal function of the PAN is to transduce and amplify a signal. Such catecholamine–PANi interactions can affect the charge–carrier density of the conjugated

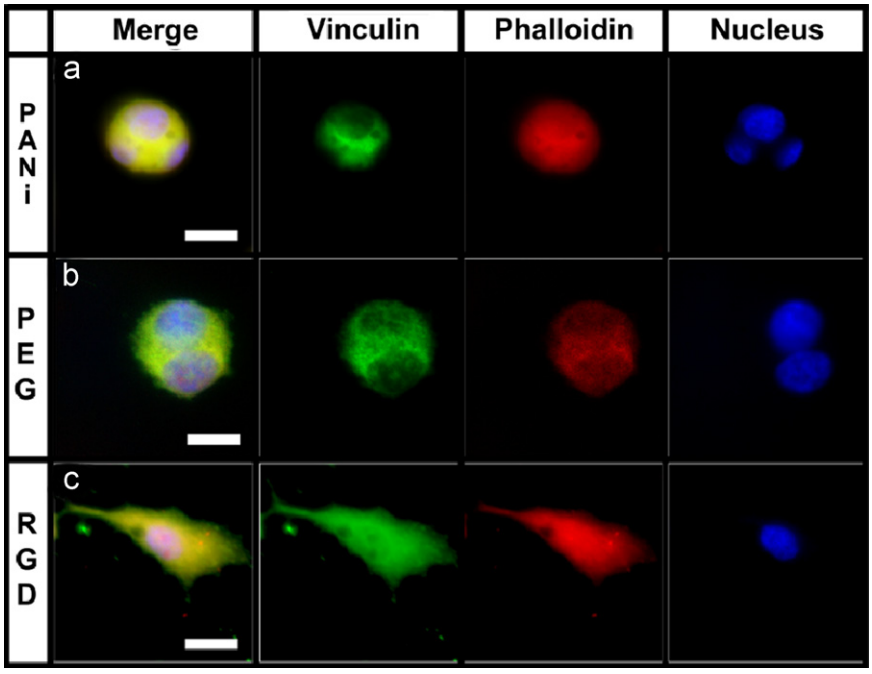

Fig. 4. Representative fluorescence microscopy pictures displaying overlay of green staining vinculin, red staining actin, and blue staining the nucleus, separate views of vinculin, actin, and nucleus image. (a) pristine PANi, (b) PEG–treated PANi, (c) RGD–immobilized PANi pattern. Scale bar = 10 μm. (For interpretation of the references to colour in this figure legend, the reader is referred to the web version of this article.)

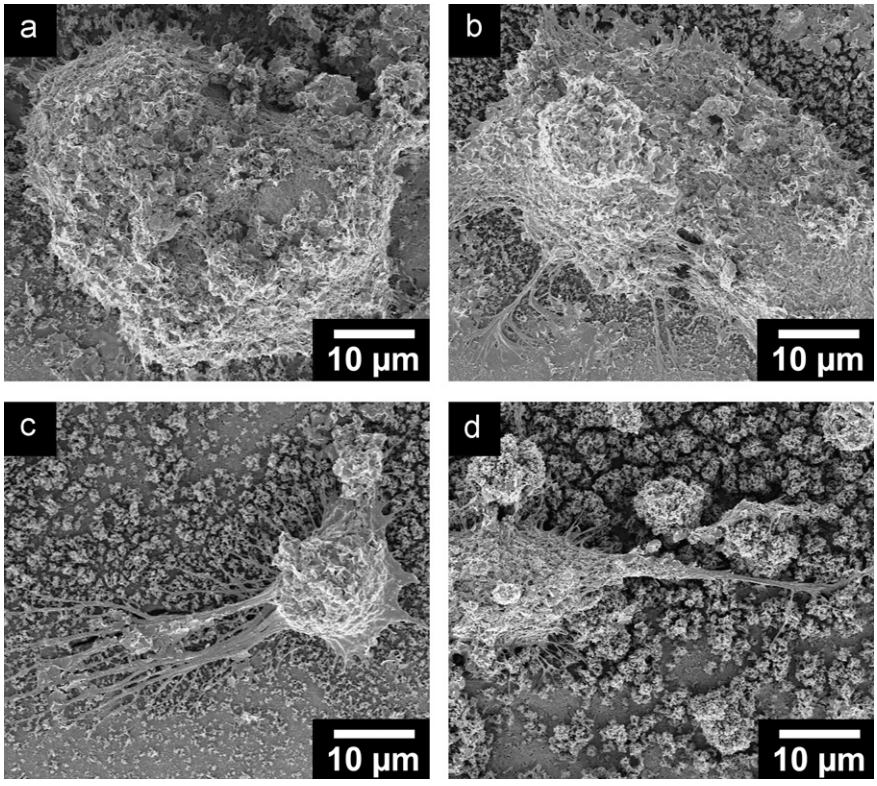

Fig. 5. SEM images of PC-12 cell adhered on (a) pristine PANi pattern, (b) PEG–treated PANi pattern and (c,d) RGD–immobilized PANi pattern.

PANi patterns, and thus may allow label–free recognition of neurotransmitter secretion from neurons. Such catecholamine–PANi interactions can affect the charge–carrier density of the conjugated PANi patterns, and thus may allow label–free recognition of neurotransmitter secretion from neurons. The use of potassium ions and calcymycin together triggered exocytosis due to forming calcium ion channels. These spikes are similar to those previously reported for recordings of catecholamine release [42]. Each spike indicates the exocytosis of catecholamines from live cells. As a control, catecholamines were inserted

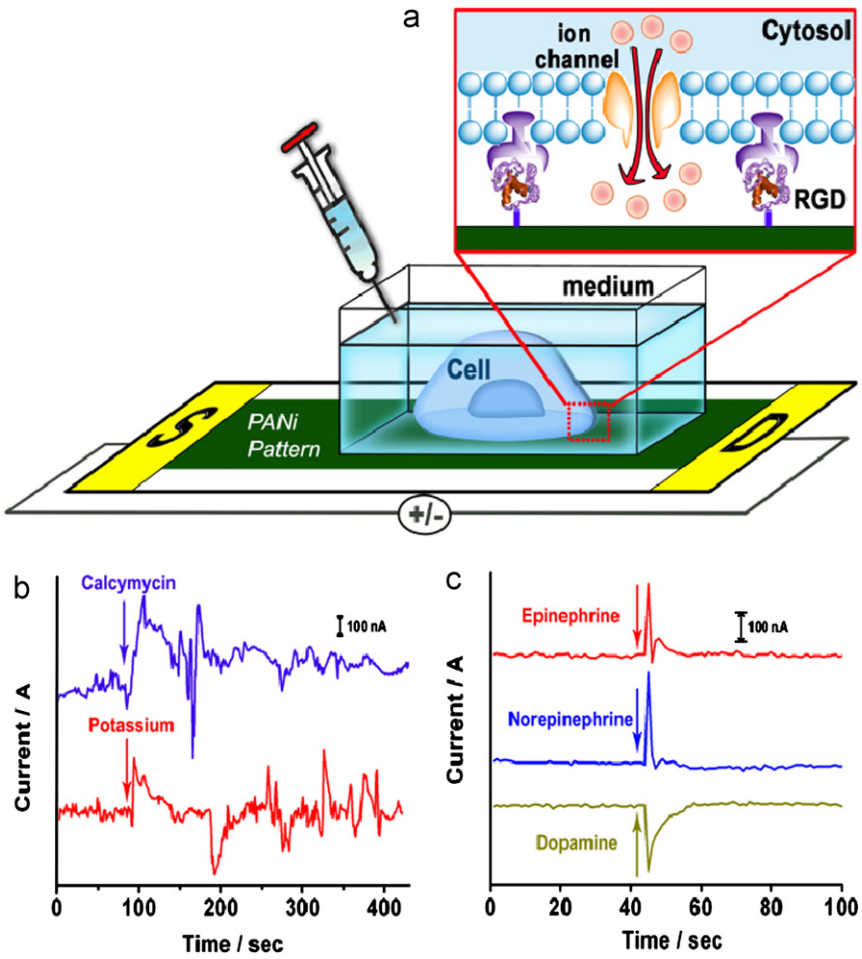

Fig. 6. (a) Schematic diagram of a biomolecule detection system from live cells. (b) Live cell response of RGD–immobilized PANi pattern sensors measured at V_{SD}=50 mV; currents change upon addition of 1 μm potassium ion and calcymycin solution (Arrows indicate inserting time). (c) Response of RGD–immobilized PANi pattern upon exposure of 1 μm epinephrine, norepinephrine, and dopamine without cell (Arrows indicate inserting time).

onto a PANi pattern without cells (Fig. 6c). Epinephrine and norepinephrine induced a sharp current spike, indicating the local discharge of catecholamines caused a transient increase in the PANi pattern current, similar to the data in Fig. 6b. Furthermore, a negative change in current was observed after the insertion of dopamine; thus, dopamine may be distinguished from other catecholamines. Real-time responses of the RGD-modified PANi pattern upon exposure to dopamine at various concentrations were examined (Fig. S5). The response of the PANi pattern upon sequential exposure to dopamine (2, 20, 40, and 1000 nM) exhibits excellent sensitivity, rapid response, and recovery time. The response times were less than 1 s, and the recovery times were less than 50 s; the response and recovery times are respectively defined as the times required for sensor signals to reach 90% of the saturation and original values [2]. The PANi pattern showed a concentration-dependent increase in the current when exposed to dopamine. The current increase was not attributed to electrochemical oxidation of dopamine, because the applied voltage was below its oxidation potential. It is believed that the current increase is due to a change in the charge-transport behavior of the PANi patterns elicited by the dopamine attachment to the pattern. Limit of detection of the PANi pattern toward dopamine was ca. 2 nM. The signals generated by these catecholamines and secretagogues may be distinguished from molecules secreted constitutively from live cells because constitutive secretion is a slow, constant process compared with rapid exocytosis. Consequently, the RGD–immobilized PANi pattern allowed translation and amplification of exocytized molecules into detectable signals.

4. Conclusions

We demonstrated the feasibility of neurotransmitter detection from live cells using inkjet-printed and RGD–immobilized PANi patterns. This strategy enabled the facile fabrication of a flexible cell patterning and sensing substrate with high selectivity and interactive exocytosed molecule detection. The selective cell attachment ratio on the PANi patterns increased with changing the surface of PANi patterns from pristine to PEG and RGD, and increasing RGD concentration. The focal adhesion of cells on RGD–immobilized PANi patterns was observed. The PANi pattern sensor provided real-time and sensitive measurements from live cells. Considering these facts, our RGD peptide–immobilized PANi pattern sensing system offers a new method for flexible selective cell patterning with focal adhesion and the detection of exocytized biomolecules.

Acknowledgments

This research was supported by WCU (World Class University) program through the National Research Foundation of Korea

funded by the Ministry of Education, Science and Technology (R31-10013).

Appendix A. Supporting information

Supplementary data associated with this article can be found in the online version at http://dx.doi.org/10.1016/j.talanta.2012.10.050.

References

[1] H. Yoon, J. Jang, Adv. Funct. Mater. 19 (2009) 1567–1576.
[2] H. Yoon, S.H. Lee, O.S. Kwon, H.S. Song, E.H. Oh, T.H. Park, J. Jang, Angew. Chem. Int. Ed. 48 (2009) 2755–2758.
[3] W.-K. Oh, S. Kim, H. Yoon, J. Jang, Small 6 (2010) 872–879.
[4] J.D. Kim, J.S. Choi, B.S. Kim, Y. Chan Choi, Y.W. Cho, Polymer (Guildf) 51 (2010) 2147–2154.
[5] I. Willner, B. Basnar, B. Willner, Adv. Funct. Mater. 17 (2007) 702–717.
[6] Y.-S. Hsiao, C.-C. Lin, H.-J. Hsieh, S.-M. Tsai, C.-W. Kuo, C.-W. Chu, P. Chen, Lab. Chip. 11 (2011) 3674–3680.
[7] J. Jang, S. Ko, Y. Kim, Adv. Funct. Mater. 16 (2006) 754–759.
[8] R.A. Green, N.H. Lovell, G.G. Wallace, L.A. Poole-Warren, Biomaterials 29 (2008) 3393–3399.
[9] T. Ahuja, I.A. Mir, D. Kumar Rajesh, Biomaterials 28 (2007) 791–805.
[10] J. Jang, J. Ha, J. Cho, Adv. Mater. 19 (2007) 1772–1775.
[11] J. Cho, K.-H. Shin, J. Jang, Synth. Met. 160 (2010) 1119–1125.
[12] J. Cho, K.-H. Shin, J. Jang, Thin Solid Films 518 (2010) 5066–5070.
[13] Y.H. Yun, B.K. Lee, J.S. Choi, S. Kim, B. Yoo, Y.S. Kim, K. Park, Y.W. Cho, Anal. Sci. 27 (2011) 375–379.
[14] W.S. Choi, D. Ha, S. Park, T. Kim, Biomaterials 32 (2011) 2500–2507.
[15] Y.-K. Kim, S.-R. Ryoo, S.-J. Kwack, D.-H. Min, Angew. Chem. Int. Ed. 48 (2009) 3507–3511.
[16] N.N. Mallikarjuna, A. Venkataraman, Talanta 60 (2003) 139–147.
[17] E. Bystrenova, M. Jelitai, I. Tonazzini, A.N. Lazar, M. Huth, P. Stoliar, C. Dionigi, M.G. Cacace, B. Nickel, E. Madarasz, F. Biscarini, Adv. Funct. Mater. 18 (2008) 1751–1756.
[18] J. Yu, Z. Liu, M. Yang, A. Mak, Talanta 80 (2009) 189–194.
[19] T. Ekblad, L. Faxälv, O. Andersson, N. Wallmark, A. Larsson, T.L. Lindahl, B. Liedberg, Adv. Funct. Mater. 20 (2010) 2396–2403.
[20] H.-W. Chien, T.-Y. Chang, W.-B. Tsai, Biomaterials 30 (2009) 2209–2218.
[21] C.Y. Tay, M. Pal, H. Yu, W.S. Leong, N.S. Tan, K.W. Ng, S. Venkatraman, F. Boey, D.T. Leong, L.P. Tan, Small 7 (2011) 1416–1421.
[22] S. Namgung, T. Kim, K.Y. Baik, M. Lee, J.M. Nam, S. Hong, Small 7 (2011) 56–61.
[23] S. Kalinina, H. Gliemann, M. López-García, A. Petershans, J. Auernheimer, T. Schimmel, M. Bruns, A. Schambony, H. Kessler, D. Wedlich, Biomaterials 29 (2008) 3004–3013.
[24] M.D. Pierschbacher, E. Ruoslahti, Nature 309 (1984) 30–33.
[25] M. Kantlehner, P. Schaffner, D. Finsinger, J. Meyer, A. Jonczyk, B. Diefenbach, B. Nies, G. Hölzemann, S.L. Goodman, H. Kessler, Chem. Bio. Chem. 1 (2000) 107–114.
[26] Y. Ikada, Biomaterials 15 (1994) 725–736.
[27] B.G. Keselowsky, D.M. Collard, A.J. Garcı´a, Biomaterials 25 (2004) 5947–5954.
[28] C.-W. Wang, C.-Y. Pan, H.-C. Wu, P.-Y. Shih, C.-C. Tsai, K.-T. Liao, L.-L. Lu, W.-H. Hsieh, C.-D. Chen, Y.-T. Chen, Small 3 (2007) 1350–1355.
[29] H.G. Sudibya, J. Ma, X. Dong, S. Ng, L.-J. Li, X.-W. Liu, P. Chen, Angew. Chem. Int. Ed. 48 (2009) 2723–2726.
[30] C.M. Correa, R. Faez, M.A. Bizeto, F.F. Camilo, RSC Adv. 2 (2012) 3088–3093.
[31] V. Brunetti, G. Maiorano, L. Rizzello, B. Sorce, S. Sabella, R. Cingolani, P.P. Pompa, Proc. Natl. Acad. Sci. 107 (2010) 6264–6269.
[32] T. Cohen-Karni, Q. Qing, Q. Li, Y. Fang, C.M. Lieber, Nano Lett. 10 (2010) 1098–1102.
[33] T. Cohen-Karni, B.P. Timko, L.E. Weiss, C.M. Lieber, Proc. Natl. Acad. Sci. 106 (2009) 7309–7313.
[34] A.J. Hilmer, M.S. Strano, Nat. Nano. 5 (2010) 481–482.
[35] M. Glaser, M. Morrison, M. Solbakken, J. Arukwe, H. Karlsen, U. Wiggen, S. Champion, G.M. Kindberg, A. Cuthbertson, Bioconjugate Chem. 19 (2008) 951–957.
[36] J. Hyun, H. Ma, P. Banerjee, J. Cole, K. Gonsalves, A. Chilkoti, Langmuir 18 (2002) 2975–2979.
[37] H.S. Seo, Y.M. Ko, J.W. Shim, Y.K. Lim, J.-K. Kook, D.-L. Cho, B.H. Kim, Appl. Surf. Sci. 257 (2010) 596–602.
[38] S.T. Khew, Q.J. Yang, Y.W. Tong, Biomaterials 29 (2008) 3034–3045.
[39] M.-S. Qiu, S.H. Green, Neuron 9 (1992) 705–717.
[40] J. Malmstroöm, J. Lovmand, S. Kristensen, M. Sundh, M. Duch, D.S. Sutherland, Nano Lett. 11 (2011) 2264–2271.
[41] J. Malmström, B. Christensen, H.P. Jakobsen, J. Lovmand, R. Foldbjerg, E.S. Sørensen, D.S. Sutherland, Nano Lett. 10 (2010) 686–694.
[42] X. Liu, S. Barizuddin, W. Shin, C.J. Mathai, S. Gangopadhyay, K.D. Gillis, Anal. Chem. 83 (2011) 2445–2451.